AMERICAN SOCIETY FOR MICROBIOLOGY | Journal of Bacteriology®

RESEARCH ARTICLE

The Chemoreceptor Sensory Adaptation System Produces Coordinated Reversals of the Flagellar Motors on an *Escherichia coli* Cell

Yumiko Uchida,[a] Tatsuki Hamamoto,[a]* Yong-Suk Che,[a] Hiroto Takahashi,[b] John S. Parkinson,[c] Akihiko Ishijima,[a] Hajime Fukuoka[a]

[a]Graduate School of Frontier Biosciences, Osaka University, Osaka, Japan
[b]Institute of Multidisciplinary Research for Advanced Materials, Tohoku University, Miyagi, Japan
[c]School of Biological Sciences, University of Utah, Salt Lake City, Utah, USA

ABSTRACT In isotropic environments, an *Escherichia coli* cell exhibits coordinated rotational switching of its flagellar motors, produced by fluctuations in the intracellular concentration of phosphorylated CheY (CheY-P) emanating from chemoreceptor signaling arrays. In this study, we show that these CheY-P fluctuations arise through modifications of chemoreceptors by two sensory adaptation enzymes: the methyltransferase CheR and the methylesterase CheB. A cell containing CheR, CheB, and the serine chemoreceptor Tsr exhibited motor synchrony, whereas a cell lacking CheR and CheB or containing enzymatically inactive forms did not. Tsr variants with different combinations of methylation-mimicking Q residues at the adaptation sites also failed to show coordinated motor switching in cells lacking CheR and CheB. Cells containing CheR, CheB, and Tsr [NDND], a variant in which the adaptation site residues are not substrates for CheR or CheB modifications, also lacked motor synchrony. TsrΔNWETF, which lacks a C-terminal pentapeptide-binding site for CheR and CheB, and the ribose-galactose receptor Trg, which natively lacks this motif, failed to produce coordinated motor switching, despite the presence of CheR and CheB. However, addition of the NWETF sequence to Trg enabled Trg-NWETF to produce motor synchrony, as the sole receptor type in cells containing CheR and CheB. Finally, CheBc, the catalytic domain of CheB, supported motor coordination in combination with CheR and Tsr. These results indicate that the coordination of motor switching requires CheR/CheB-mediated changes in receptor modification state. We conclude that the opposing receptor substrate-site preferences of CheR and CheB produce spontaneous blinking of the chemoreceptor array's output activity.

IMPORTANCE Under steady-state conditions with no external stimuli, an *Escherichia coli* cell coordinately switches the rotational direction of its flagellar motors. Here, we demonstrate that the CheR and CheB enzymes of the chemoreceptor sensory adaptation system mediate this coordination. Stochastic fluctuations in receptor adaptation states trigger changes in signal output from the receptor array, and this array blinking generates fluctuations in CheY-P concentration that coordinate directional switching of the flagellar motors. Thus, in the absence of chemoeffector gradients, the sensory adaptation system controls run-tumble swimming of the cell, its optimal foraging strategy.

KEYWORDS signal transduction, chemotaxis, receptor, methylation, CheY, *E. coli*

Escherichia coli cells swim by rotating left-handed helical flagellar filaments. Counterclockwise (CCW) rotation produces forward swimming; clockwise (CW) rotation triggers random turning movements, called tumbles (1). *E. coli* cells swimming in a liquid

Editor Mohamed Y. El-Naggar, University of Southern California

Address correspondence to Hajime Fukuoka, f-hajime@fbs.osaka-u.ac.jp.

*Present address: Tatsuki Hamamoto, Okinawa Institute of Science and Technology Graduate University, Okinawa, Japan.

The authors declare no conflict of interest.

Received 21 July 2022
Accepted 1 November 2022
Published 30 November 2022

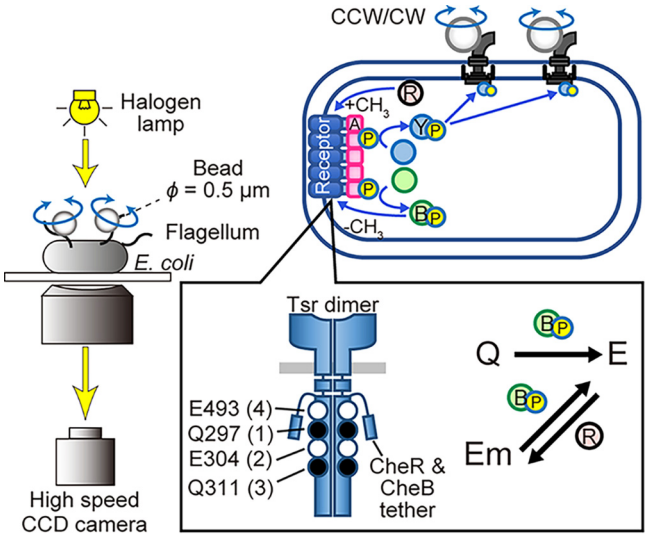

FIG 1 An overview of the method used to follow steady-state switching of flagellar motors and the *E. coli* sensory adaptation system. A cell was stuck to a coverslip, and polystyrene beads (ϕ = 0.5 μm) were attached to the sticky flagellar stubs to observe the angular velocity of each motor from the position of its bead. The signaling activity of the polar chemoreceptor array within the cell modulates the autophosphorylation of CheA (A), which in turn donates its phosphoryl groups (P) to CheY (Y-P) and CheB (B-P). Phosphorylated CheY (CheY-P) interacts with the flagellar motors to promote clockwise (CW) rotation. CheB-P deamidates and demethylates adaptation site residues in the receptor signaling domain (in Tsr: Q297, E304, Q311, and E493); phosphorylation of CheB enhances these activities. CheB preferentially acts on receptors in the on state to shift their output toward the off state. CheR preferentially methylates available adaptation sites on receptors in the off state to shift their output toward the on state. CCD, charge-coupled device; CCW, counterclockwise.

environment track and navigate chemical gradients with high precision, a behavior termed chemotaxis (2, 3). To monitor attractant or repellent chemicals in its environment, *E. coli* uses transmembrane chemoreceptors known as methyl-accepting chemotaxis proteins (MCPs). *E. coli* has four canonical MCPs for sensing attractant nutrients: Tsr (serine), Tar (aspartate and maltose), Tap (dipeptides), and Trg (ribose and galactose). These chemoreceptors have a common functional architecture and transmit sensory messages to the flagellar motors through a two-component phosphorelay (4).

MCPs assemble large signaling arrays at the cell pole(s) through binding interactions with two cytoplasmic proteins (Fig. 1): a histidine autokinase CheA and a scaffolding protein CheW that couples CheA activity to receptor control (4–7). Receptor arrays modulate the autophosphorylation activity of CheA to control the flux of phosphoryl groups from CheA to the response regulator CheY. Phosphorylated CheY (CheY-P) is the intracellular messenger that binds to a flagellar motor to induce CW rotation (8–13). CheY-P molecules appear to reach the flagellar motors through intracellular diffusion (14). CheZ, a dedicated CheY-P phosphatase, degrades the CW signal, but it is located mainly at the polar receptor arrays through interaction with a variant form of CheA, $CheA_{short}$ (15, 16). Thus, CheY-P is generated at receptor arrays, and the majority of CheY-P is degraded by CheZ before it can escape the array (14).

Two MCP-specific chemotaxis proteins, CheR and CheB, mediate sensory adaptation in the *E. coli* chemotaxis system (Fig. 1). CheR is a methyltransferase that converts specific glutamate (E) residues in MCPs to methylated glutamate (Em) residues. CheB is a methylesterase that converts Em residues to E residues (17); that activity is enhanced upon phosphorylation of CheB by CheA. The serine chemoreceptor Tsr contains five methyl-accepting sites per subunit: Q297, E304, Q311, E493, and E502 (this fifth site is a minor one and was not manipulated in this study). Two of the residues are encoded as glutamine (Q), which is known to mimic the effect of an Em residue on MCP signaling activity (18–21). Under steady-state conditions, the Q residues in newly synthesized Tsr molecules are irreversibly converted to E residues by deamidase activity of CheB,

yielding five E sites available for reversible modification by CheR and CheB (Fig. 1). CheR preferentially acts on receptors in the kinase-off state; methylation shifts their output toward the kinase-on state. In contrast, CheB preferentially acts on receptors in the kinase-on state and demethylation shifts their output toward the off state; therefore, the methylation level in MCP is feedback controlled according to its own activity. The interplay of CheR and CheB action comprises a feedback system of sensory adaptation control of receptor signaling activity (22–24).

Previously, we demonstrated that under steady-state conditions with no external chemotactic stimuli, two flagellar motors on the same *E. coli* cell coordinately switched their rotational direction through increases and decreases in CheY-P concentration. We proposed that fluctuations in CheY-P concentration might be generated by spontaneous activation and inactivation of signal activity in the receptor array ("array blinking") (14, 25). This signal fluctuation depends on the signal-generating and signal-destroying reactions in the polar receptor array and on diffusion of the signaling molecule phospho-CheY between the array and the flagellar motors. In the present study, we investigated whether the sensory adaptation enzymes CheR and CheB might be responsible for blinking of receptor array activity. We found that the coordination of flagellar motor switching events required both CheR and CheB enzyme activities and modification-competent MCP substrates. From these results, we conclude that even in the absence of chemotactic stimuli, the sensory adaptation enzymes create transient fluctuations in the average modification states of receptors that underlie blinking of array activity, thereby producing fluctuations in CheY-P concentration that synchronize switching of flagellar motors on the cell.

RESULTS

CheR and CheB are required for synchronous motor switching. To investigate the role of the sensory adaptation enzymes in coordinated rotational switching of flagellar motors on a cell, we used a strain (EFS073) with chromosomal deletions of the MCP, *cheR*, and *cheB* genes and supplied various combinations of Tsr, CheR, and CheB proteins with compatible expression plasmids, as described in the Materials and Methods section. We observed the rotation of two motors on the same cell with small beads attached to their flagellar filaments, as illustrated in Fig. 1 (see also Materials and Methods). The rotational motion of each bead was followed with a high-speed charge-coupled device (CCD) camera to obtain a time trace of the rotational velocity and directional switching of the two motors (14, 25).

A strain containing wild-type Tsr, CheR, and CheB appeared to switch motor rotation synchronously, as we previously reported (14, 25) (Fig. 2A). To assess switching coordination, a correlation analysis was performed of the rotational time traces for the two motors (Materials and Methods). The analysis showed a major peak near 0 s (Fig. 2B), indicating that the two motors switched in synchrony. This coordination prevailed in 14 of 15 cells that we observed (Fig. 2C, gray dotted lines) and was still apparent in the averaged correlation profile (Fig. 2C, red line). These results indicate that cells having CheR/CheB and only one type of receptor (Tsr) show coordinated switching in the absence of chemoeffector stimuli, as we found previously for cells with all-MCP arrays (14, 25). We note that the Tsr-only CheR/CheB cells were chemotactic in semisolid agar assays, indicating complementation activity of the plasmid-carried genes (Fig. S1).

A strain containing wild-type Tsr, but neither CheR nor CheB, failed to switch its flagellar motors coordinately (Fig. 2D and 2E). Of 14 cells analyzed, all lacked motor synchrony (Fig. 2F). The Tsr protein in these cells carried a [QEQE] pattern at methylation sites 1 to 4, so in the absence of CheR and CheB, the two E sites would remain unmethylated, and the two Q sites would mimic Em sites. Evidently Tsr with an invariant [QEQE] modification pattern cannot support motor synchrony, but might Tsr with a different modification pattern behave differently? To explore this possibility, we examined the rotation patterns of cells expressing various Q/E variants of Tsr. In cells lacking CheR and CheB, no Tsr Q/E variants supported motor synchrony (Fig. S2B), whereas

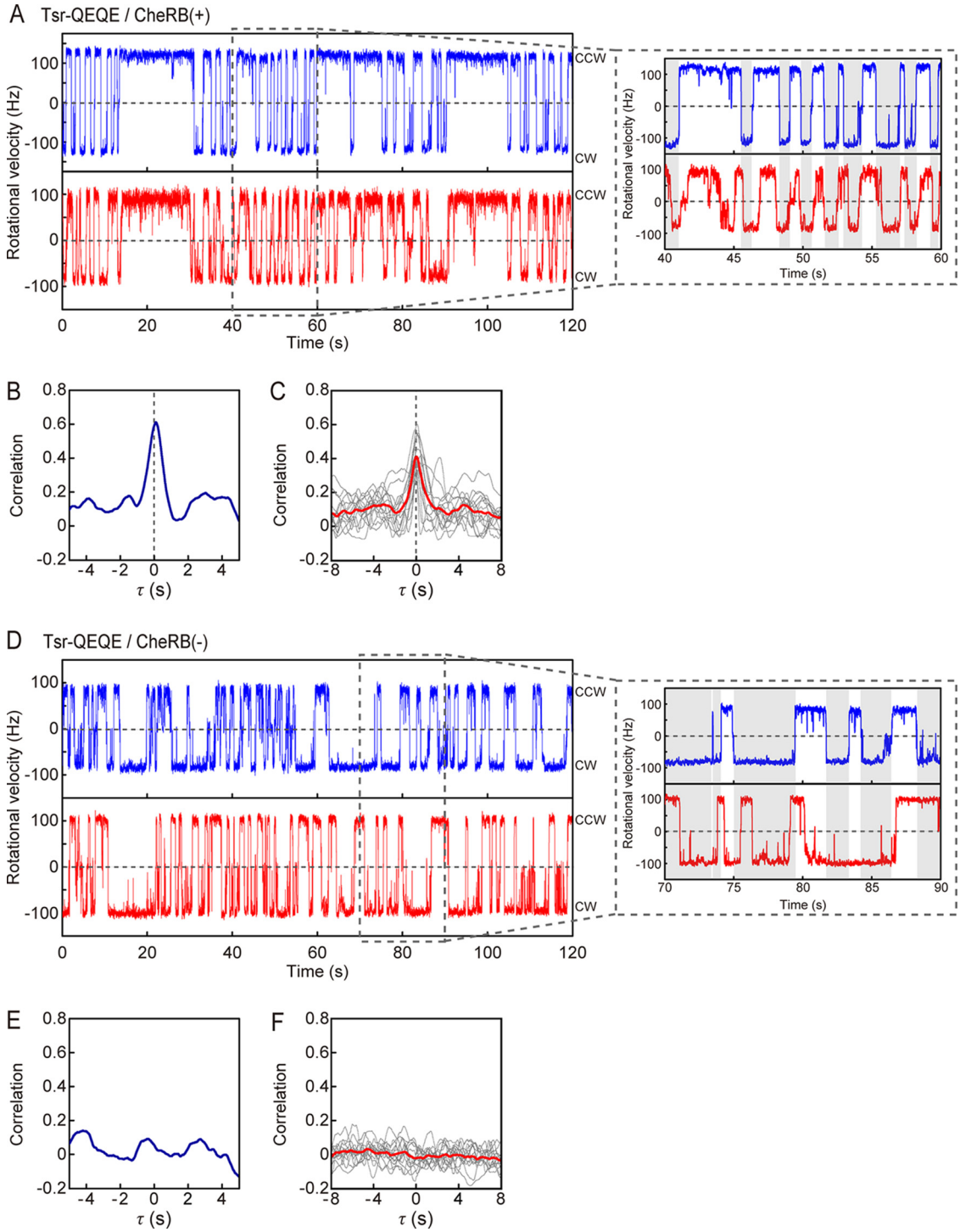

FIG 2 (A, left) Motor switching patterns of cells with and without CheR/CheB. Time traces of the rotational directions of two motors (blue, red) on an EFS073 cell carrying plasmids pPA114 (wild-type Tsr) and pFSRB1 (wild-type CheR and CheB). (Right) The time traces over a short time period. The gray areas mark episodes of clockwise (CW) rotation in the upper trace. (B) A cross-correlation profile for the time traces of the two motors in panel A. (C) Gray lines indicate individual correlations for 15 cells as in panel A; the red line shows the average trace of those correlation analyses. (D) Time traces of the rotational directions of two different motors on an EFS073 cell carrying plasmids pPA114 (wild-type Tsr) and pBAD24 (vector; no CheR and no CheB). (E) A cross-correlation profile for the time traces of the two motors in (D). (F) Individual (gray) and average (red) correlations for 14 cells as in panel D. All correlation analyses were performed for time traces over 60 to 120 s.

cells containing the CheR and CheB enzymes and the same Tsr variants showed coordinated motor switching (Fig. S2C). These results indicate that homogeneous arrays of receptors in any fixed modification state could not coordinate the switching of two motors on the same cell. Thus, one or both of the sensory adaptation enzymes is essential for coordinated motor switching.

We note that in all seven cell lines containing a single Tsr modification variant, the variance of CW bias between two motors was low in the presence of CheR and CheB due to synchronous switching (Fig. S3). In contrast, in the absence of CheR and CheB, the variance in CW bias between the two motors was much greater. Motor switching is known to show a steep sigmoidal dependence on CheY-P concentration, with reversal changes centered at $\sim$3 μM CheY-P (26). In cells containing CheR and CheB, synchronous motor switching would require large changes in CheY-P concentration (e.g., from 1 to 6 μM). The absence of switching coordination in cells lacking CheR and CheB (Fig. 2) implies that their receptor array does not produce large changes in CheY-P concentration. However, if the CheY-P concentration in cells lacking the adaptation enzymes hovers near 3 μM, small fluctuations in CheY-P level would lead to large variations in CW bias between two motors in the same cell.

Both CheR and CheB activities are required for synchronous motor switching. To investigate whether the methylation activity of CheR and/or the demethylation activity of CheB are required for coordinated motor switching, we investigated the coordination between motors in cells producing wild-type Tsr and mutants of CheR and CheB with catalytic defects. CheR-R53A and CheB-H190Y lack enzymatic activity, but both mutant proteins can still localize at receptor clusters (27, 28). An EFS073 cell containing wild-type Tsr receptors, CheR-R53A, and CheB-H190Y failed to show motor synchrony (Fig. 3A to 3C). This result held for cells that we observed (10/10 cells) (Fig. 3D). (The relative expression levels of the CheB and CheR variants are shown in Fig. S4). These results indicate that either the methylation activity of CheR, the demethylation activity of CheB, or both activities are required to coordinate the switching between flagellar motors on a cell.

CheR and CheB must covalently modify receptors to produce motor synchrony. To determine whether CheR/CheB-promoted receptor modifications are essential for coordinated motor switching, we investigated switching patterns in EFS073 cells that contained wild-type CheR and CheB proteins, but in combination with a Tsr [NDND] variant receptor that has no suitable substrate sites for CheR or CheB modifications and has similar signaling property to Tsr-QEQE (19). Such a cell did not show coordinated switching events (Fig. 4A to 4C), a result that held for cells that we observed (12/12 cells) (Fig. 4D). The expression level of the Tsr [NDND] variant was comparable to that of wild-type Tsr (Fig. S4). We conclude that CheR and/or CheB must modify receptor molecules to cause synchronous switching of the cell's flagellar motors.

CheR and CheB must bind to receptors to produce motor synchrony. CheR and CheB are known to bind to a C-terminal pentapeptide sequence (NWETF) present on Tsr and Tar molecules. Receptor binding substantially enhances the ability of CheR and CheB to encounter and modify adaptation site targets (29–31). To investigate whether the NWETF pentapeptide of Tsr is required for coordinated motor switching, we investigated the rotation patterns of cells containing wild-type CheR and CheB proteins in combination with mutant Tsr receptors lacking the NWETF motif (TsrΔNWETF).

We confirmed that CheR could not bind to TsrΔNWETF by imaging Venus-CheR in EFS073 cells containing wild-type Tsr or TsrΔNWETF. Wild-type Tsr cells exhibited polar localization of Venus-CheR (Fig. 5A), but TsrΔNWETF cells did not (Fig. 5B), suggesting that CheR cannot interact effectively with TsrΔNWETF. We also confirmed, as expected, that both wild-type and TsrΔNWETF formed polar receptor arrays by imaging green fluorescent protein (GFP)-CheW, an essential component of receptor signaling complexes (Fig. 5A and 5B).

Next, we compared the coordination of motor switching in cells containing plasmid-expressed wild-type Tsr or TsrΔNWETF. For these measurements, we used a strain (EFS069) devoid of all receptor genes but producing CheR and CheB from the wild-

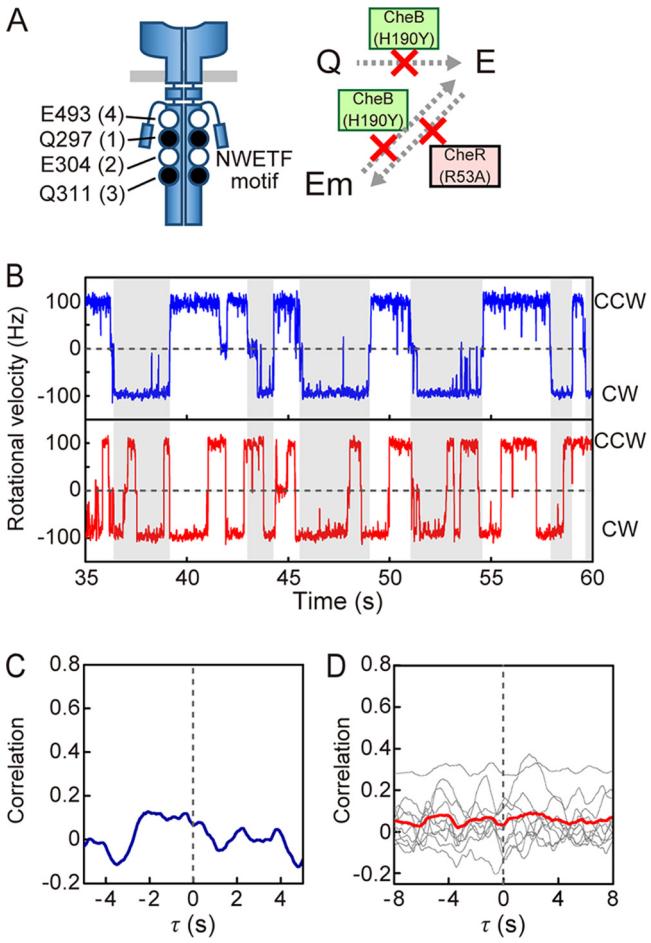

FIG 3 Motor switching patterns of cells containing enzymatically inactive CheR and CheB. (A) Schematic diagram of proteins in the cells. (B) Time traces of the rotational directions of two different motors on an EFS073 cell carrying plasmids pPA114 (wild-type Tsr) and pFSRB4 (CheR-R53A and CheB-H190Y). Portion of the time traces are shown here; see Fig. S5 for the full 60-s time trace. Gray areas indicate CW rotation episodes in the upper trace. (C) Cross-correlation profile for the two motors in panel B over 60 s. (D) Individual (gray) and average (red) correlations for 10 cells as in panel B.

type chromosomal genes. We observed motor synchrony in 17 of 18 cells containing wild-type Tsr (Fig. 5C and 5D). However, 13 of 13 cells containing TsrΔNWETF did not show coordinated motor switching (Fig. 5E and 5F). These results indicate that the Tsr NWETF motif was essential for synchronous switching.

To further verify the requirement of the receptor NWETF pentapeptide for switching coordination, we measured the rotation patterns of cells containing the wild-type Trg receptor, which naturally lacks the NWETF motif and of cells containing a Trg with an appended NWETF pentapeptide of Tsr (Trg-NWETF), which enhances the ability of Trg to function in the absence of other NWETF-containing receptor types (32). Both Trg and Trg-NWETF formed polar clusters with the GFP-CheW reporter, demonstrating formation of signaling arrays (Fig. 5G and 5H). However, the Venus-CheR reporter did not bind to wild-type Trg clusters (Fig. 5G) but did bind to Trg-NWETF clusters (Fig. 5H). In 10 of 10 cells expressing wild-type Trg, we observed their motors to rotate only in the CCW direction (Fig. 5I). The low CW motor bias in cells with wild-type Trg as their only receptor type was previously reported by Feng et al. (32). In contrast, Trg-NWETF cells exhibited rotational switching of their flagellar motors (Fig. 5J), and switching of two motors on the same cell was coordinated in 9 of 12 cells that we observed (Fig. 5K). Thus, addition of the NWETF motif to Trg conferred coordinate motor switching behavior on the cells. The relative expression levels for all MCP variants are given in Fig. S4.

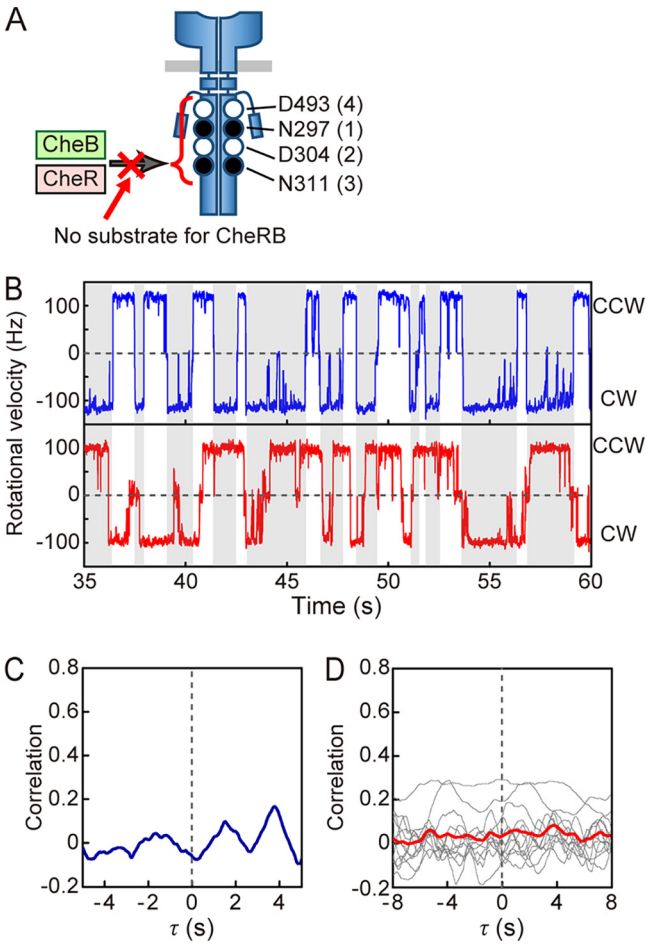

FIG 4 Motor switching patterns of cells containing receptors with unmodifiable adaptation site residues. (A) Schematic diagram of proteins in the cells. (B) Time traces of the rotational directions of two different motors on an EFS073 cell carrying plasmids pUCI52 (Tsr [NDND]) and pFSRB1 (wild-type CheR and CheB). Portions of the time traces are shown here; see Fig. S6 for the full 60-s time trace. Gray areas indicate CW rotation episodes in the upper trace. (C) Cross-correlation profile for the two motors in panel B over 60 s. (D) Individual (gray) and average (red) correlations for 11 cells as in panel B.

Phosphorylation of CheB is not essential for coordinated motor switching. The wild-type CheB protein contains two domains: a C-terminal catalytic domain and an N-terminal regulatory domain that modulates CheB catalytic activity. In the on-output state, receptors promote CheA autophosphorylation, which in turn leads to phosphorylation of the CheB regulatory domain and a consequent increase in CheB activity (Fig. 6A, left). To investigate whether CheB phosphorylation is required for motor coordination, we measured the switching behaviors of EFS073 cells containing wild-type Tsr, wild-type CheR, and CheBc, a mutant CheB protein that lacks the regulatory domain. The CheBc protein has only the C-terminal catalytic domain, but it is able to promote sensory adaptation to a tumble-enhancing repellent stimulus (33) (Fig. 6A, right). We found that such a cell exhibited motor synchrony (Fig. 6B and C), and this result held for 12 of 12 cells that we observed (Fig. 6D). These results show that the demethylation activity of CheBc in combination with the methylation activity of CheR is sufficient to induce coordinated switching of a cell's flagellar motors; CheB phosphorylation is not essential to this process.

DISCUSSION

We have investigated the mechanism of intracellular signaling by the *E. coli* chemotaxis machinery by observing the rotation of two different flagellar motors on the

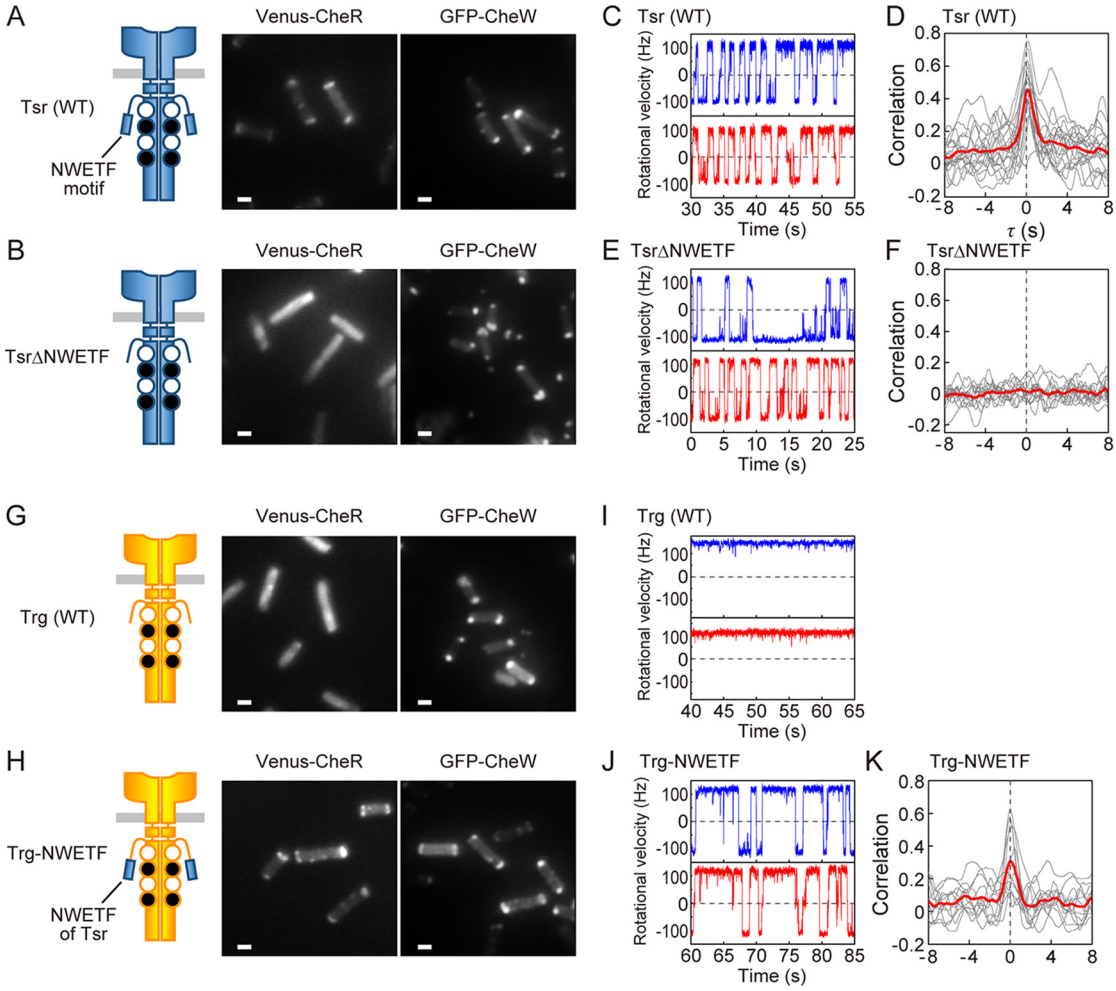

FIG 5 Motor switching patterns of cells containing receptors with or without a CheR/CheB tether (NWETF). (A) Fluorescence in EFS073 cells carrying plasmids pPA114 (wild-type [WT] Tsr) and pFSVnRB (Venus-CheR, wild-type CheB) and in EFS069 cells carrying plasmids pPA114 (wild-type Tsr) and pFSGW2 (green fluorescent protein [GFP]-CheW). (B) Fluorescence in EFS073 cells carrying plasmids pUCI30a (TsrΔNWETF) and pFSVnRB (Venus-CheR, wild-type CheB) and in EFS069 cells carrying plasmids pUCI30a (TsrΔNWETF) and pFSGW2 (GFP-CheW). (C) Rotational traces of two different motors on an EFS069 carrying plasmid pPA114 (wild-type Tsr). (D) Individual (gray) and average (red) correlations for 18 cells as in panel C. (E) Rotational traces of two different motors on an EFS069 cell carrying plasmid pUCI30a (TsrΔNWETF). (F) Individual (gray) and average (red) correlations for 13 cells as in panel E. (G) Fluorescence in EFS073 cells carrying plasmids pUCI23 (wild-type Trg) and pFSVnRB (Venus-CheR, wild-type CheB) and in EFS069 cells carrying plasmids pUCI23 (wild-type Trg) and pFSGW2 (GFP-CheW). (H) Fluorescence in EFS073 cells carrying plasmids pUCI24 (Trg-NWETF) and pFSVnRB (Venus-CheR, wild-type CheB) and in EFS069 cells carrying plasmids pUCI24 (Trg-NWETF) and pFSGW2 (GFP-CheW). (I) Rotational traces of two different motors on an EFS069 carrying plasmid pUCI23 (wild-type Trg). (J) Rotational traces of two different motors on an EFS069 cell carrying plasmid pUCI24 (Trg-NWETF). (K) Individual (gray) and average (red) correlations for 12 cells as in panel J. See Fig. S7 for the full 120-s time trace for motor switching patterns. All bars in fluorescence images are 1 μm.

same cell (14, 25). In that work, we found that rotational reversals of a cell's motors were highly correlated and consistent with spontaneous fluctuations in the level of CheY-P signaling molecules that emanate from the cell's chemoreceptor array and diffuse to the flagellar motors. This blinking of receptor array activity occurs over time scales of several hundred milliseconds and under steady-state conditions in the absence of chemoeffector gradients. In the current study, we asked whether the receptor sensory adaptation system might be responsible for the blinking behavior of the chemoreceptor array.

Receptor adaptation enzymes and blinking array outputs. We found that cells lacking CheR, the receptor methyltransferase, and CheB, the receptor demethylase/deamidase, did not blink: their flagellar motors reversed independently and asynchronously. Mutant forms of the CheR-R53A and CheB-H190Y proteins that lack enzymatic

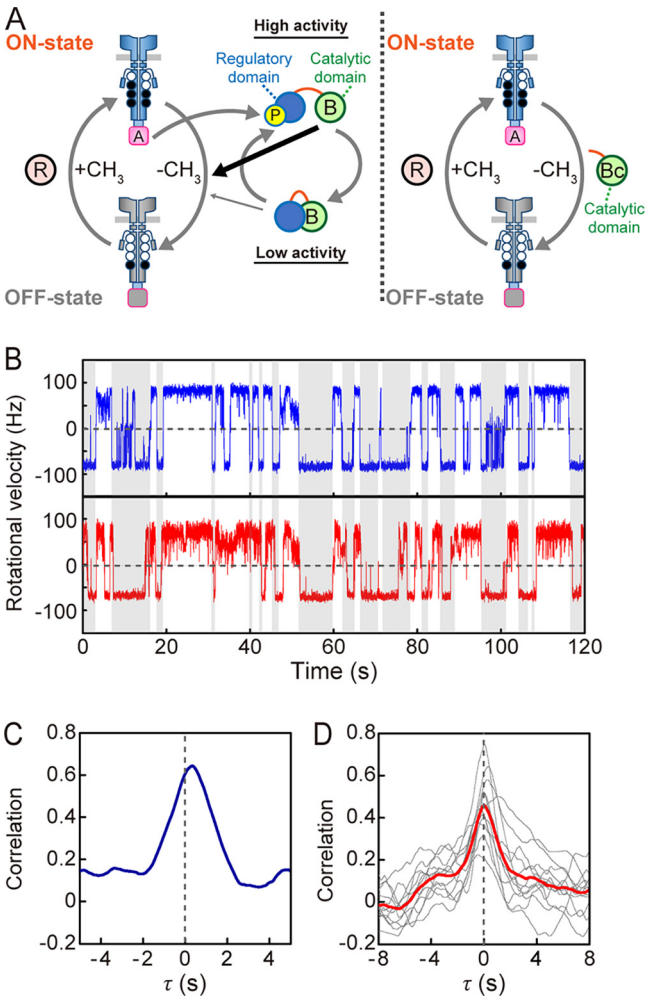

FIG 6 Motor switching patterns of cells containing CheB protein with or without the N-terminal regulatory domain. (A) Schematic diagram of proteins in the cells. (B) Time traces of the rotational directions of two different motors on an EFS073 cell carrying plasmids pPA114 (wild-type Tsr) and pUCI41 (wild-type CheR and CheBc). (C) Cross-correlation profile for the two motors in panel B. (D) Individual (gray) and average (red) correlations for 12 cells as in panel B.

activity but that retain the ability to bind to the NWETF pentapeptide found at the C terminus of the Tsr and Tar chemoreceptors also could not support blinking. The pentapeptide tether is essential for efficient CheR and CheB modifications of the chemoreceptors (29, 30). Removal of the pentapeptide from the Tsr receptor abrogated blinking, whereas appending the pentapeptide to the Trg receptor, which normally lacks the NWETF tether, enabled it to promote blinking when it was the only receptor species in the cell. These results suggest that in homogeneous environments devoid of chemoeffector gradients, chemoreceptors probably undergo methylation and demethylation reactions that promote synchronous switching of the flagellar motors.

To test the idea that a precise receptor modification state might be responsible for synchronous motor reversals, we surveyed the switching patterns of cells containing Tsr Q/E variants with different combinations of methyl-mimicking Q residues at the adaptation sites. In cells lacking the adaptation enzymes, no Tsr variant, ranging from all-E to all-Q modification states, promoted coordinated motor reversals. In cells containing CheR and CheB, all of those Tsr Q/E variants promoted array blinking. These findings suggest that array blinking requires either a heterogeneous blend of receptor modification states in the cell or fluctuations in the average receptor modification state produced by stochastic activity of the CheR and CheB enzymes.

To ask whether CheR and CheB must act enzymatically at the receptor modification sites to cause array blinking, we examined motor synchrony in cells carrying Tsr [NDND], which has signaling properties comparable to wild-type Tsr [QEQE] (19) but is not a substrate for either adaptation enzyme. Tsr [NDND] did not promote coordinated switching of the flagellar motors in cells containing CheR and CheB, confirming that enzymatic modifications of the receptor molecules underlie array blinking behavior.

Working model for blinking output in receptor arrays. Our study has demonstrated that the receptor methylation and demethylation activities of CheR and CheB are essential to produce coordinated switching of a cell's flagellar motors. Phosphorylation of CheB, which substantially enhances its enzymatic activity, was not needed for array blinking. It seems that the interplay of CheB and CheR activities is sufficient to cause coordinated switching of the flagellar motors on a cell (Fig. 6). We conclude, therefore, that the adaptation enzymes cause fluctuations in receptor modification states that result in spontaneous blinking of array activity. Under steady-state conditions, the blinking of receptor array output generates fluctuations in CheY-P production that in turn elicit synchronous reversals of a cell's flagellar motors.

Fig. 7 offers a simple mechanistic explanation for array blinking based on an integral feedback control model of Alon et al. (22) and Barkai and Leibler (23) and on Ising models of the receptor array (14, 34, 35). Although individual receptors may operate as two-state devices, the high cooperativity of signaling interactions in the chemosensory array effectively couples the output states of many receptors. Receptors in off-output domains are good substrates for CheR. The off-output domains would acquire methyl groups through CheR action until cooperatively shifting to on-output domains. Conversely, receptors in on-output domains are good substrates for CheB. The methyl groups in on-output domains will be removed through CheB action until triggering a cooperative shift to the off-output domain. In this scenario, the activity of the receptor domains blinks between on and off states through the sensory adaptation enzymes, leading to bursts of CheY-P production by the array, quickly followed by CheZ-mediated dephosphorylation.

In steady-state conditions, the duration of CCW and CW rotation episodes is on the order of several seconds (Fig. 2A). Our model proposes that array fluctuations in receptor methylation levels occur on this time scale. This is the physiologically relevant time scale for gradient-tracking behavior because the cell can use only a several-second "memory" to assess temporal changes in chemoeffector level as it swims about; any longer and Brownian motion would randomize the cell's heading (36). This time scale is considerably shorter than that required for the cell to adapt to a large, nonphysiological change in attractant concentration, which involves correspondingly large methylation increases over many minutes of experiment time (20).

Evolutionary implication of blinking receptor arrays. A swimming *E. coli* cell coordinates rotational switching of its flagellar motors (37). This means that its characteristic run-and-tumble foraging behavior caused by cellular fluctuations in CheY-P concentration arises not only through stochastic motor reversals but also through motor switching synchrony. Turner et al. (1) reported that turn angles are greater when more flagella are unwound from the bundle. Thus, coordinated switching of the flagellar motors on a cell is probably responsible for producing larger changes in swimming direction from each tumbling episode. Perhaps array blinking represents a mechanistic strategy that enables *E. coli* to explore its environment more widely by optimizing its random walk movements.

MATERIALS AND METHODS

***E. coli* strains, plasmids, and cell growth conditions.** The strains and plasmids used in this study are listed in Table S1. All strains were derived from the K-12 strain RP437, which is wild type for chemotaxis (38). The replacement of the wild-type *fli*C gene with the *fliC-sticky* gene (39) was carried out using the λ red recombinase and tetracycline sensitivity selection method (40, 41).

Amino acid replacements at Tsr methylation sites for Q/E and N/D variants were introduced by QuikChange site-directed mutagenesis (Agilent, Santa Clara, CA) or NEBuilder (New England Biolabs, Ipswich, MA) using pPA114, which encodes wild-type *tsr* as the template. Missense mutations in *cheR* and *cheB* were also created by QuikChange site-directed mutagenesis using pFSRB1 encoding wild-type *cheR* and *cheB* as the template. Plasmid pUCl41 encoding wild-type *cheR* and *cheBc*, the CheB catalytic domain (residues 147 to 349), was constructed by inverse PCR. The plasmid pUCl30a encoding TsrΔNWETF (lacking the last 11 *tsr*

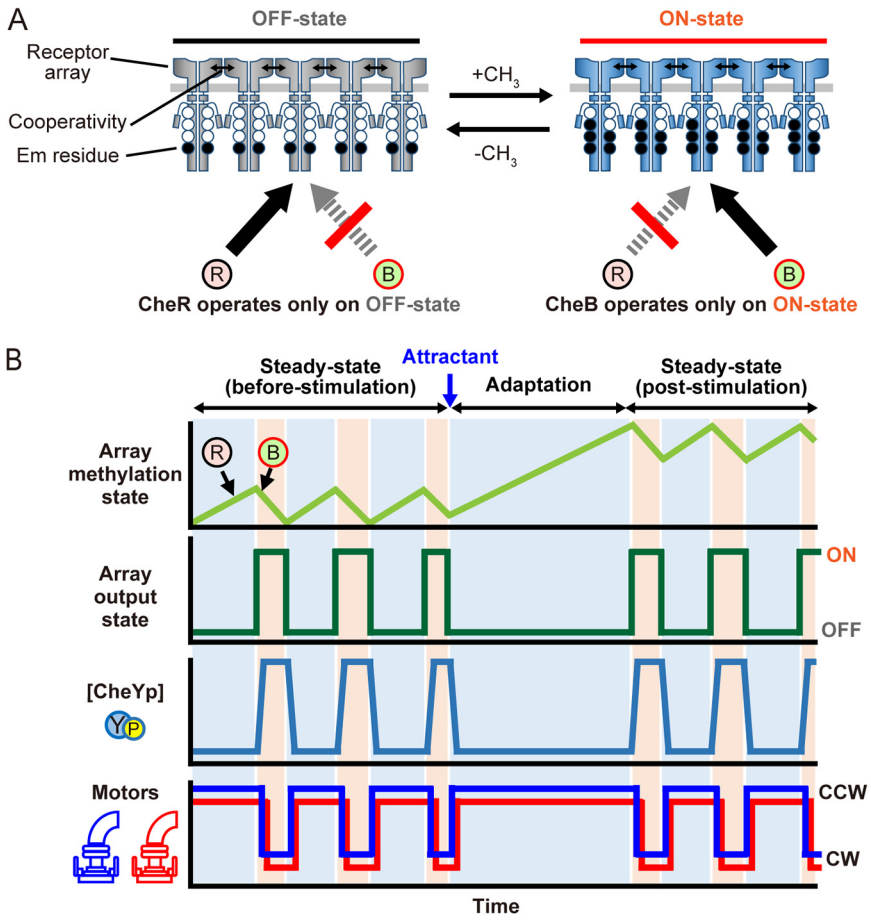

FIG 7 Model for spontaneous array blinking driven by the receptor sensory adaptation system. (A) Schematic of a receptor array in kinase-off and kinase-on-output states. CheR-mediated receptor methylation drives output toward the on state; CheB-mediated receptor demethylation drives output toward the off state. (B) The opposing receptor substrate preferences of CheR and CheB and the cooperative coupling between receptors could produce stochastic fluctuations in array activity. A predominantly off array would gain methyl groups through CheR action until cooperatively shifting to the on-output state. At that point, CheB activity would predominate, reducing array methylation until triggering a shift to the off-output state. Phospho-CheY, the CW flagellar rotation signal should track the blinking activity of the receptor array as it has a short half-life due to rapid turnover by its phosphatase CheZ. The abrupt changes in phospho-CheY level produce synchronous switching of the flagellar motors on the cell. In steady state without chemoeffectors, blinking arises from relatively small fluctuations in receptor methylation level due to the action of CheR and CheB. Upon attractant addition, the array shifts to off-output, triggering CheR-mediated receptor methylation. Upon reaching a methylation state that returns CheY-P to its prestimulus level, blinking of the now-adapted array resumes.

codons) and the plasmid pUCI24 encoding Trg-NWETF (the final 19 *tsr* codons joined to the end of the *trg* coding region) were also constructed by inverse PCR.

LB broth (1% bactotryptone [BD, Sparks, MD], 0.5% yeast extract [BD, Sparks, MD], 0.5% NaCl [Nakarai, Kyoto, Japan]) was used for culture growth, transformations, and plasmid isolation. Tryptone broth (TB) (1% bactotryptone, 0.5% NaCl) was used to grow cells for measurements of motor rotation. For all measurement, the cells were suspended in 10NaMB (10 mM potassium phosphate buffer [Wako, Osaka, Japan], pH 7.0; 0.1 mM EDTA-2K [Wako, Osaka, Japan], pH 7.0; 10 mM NaCl, 75 mM KCl [Nakarai, Kyoto, Japan]). Plasmid-bearing derivatives of strains EFS073 and EFS069 were grown at 30°C for 5.25 h in TB containing 0.5 μM salicylate to induce receptors; 0.005% arabinose to induce CheR, CheB, GFP-CheW, or Venus-CheR; 25 μg/mL chloramphenicol; and 50 μg/mL ampicillin.

Motor rotation measurements. The cells were prepared by a method similar to that described in our previous report (25). First, 1 mL of cell culture was centrifuged, and the pellet was suspended in 1 mL of 10NaMB. The cell suspension was centrifuged, and the pellet was suspended in ~300 μL of 10NaMB. The cell suspension was loaded into a sample chamber made from 18 $\times$ 18 and 24 $\times$ 50 mm coverslips with a spacer and incubated for 15 min to allow the cells to attach to the coverslip. The inside of the sample chamber was gently perfused with additional 10NaMB to remove the remaining unattached cells. A suspension of polystyrene beads with a diameter of 0.5 μm (Polysciences, 07307, PA), which was diluted 50-fold with 10NaMB immediately before loading the chamber, was injected. The mixture was

incubated for 15 min to allow the beads to attach to the flagellar filaments. The space between coverslips was gently perfused again with additional 30 μL of 10NaMB to remove unattached beads.

The rotation of the beads was measured using a microscopic system similar to the one reported previously (42). The beads were observed under phase-contrast microscopy (IX70 or IX71; Olympus, Tokyo, Japan). Phase-contrast images of the beads were recorded through a UPlanFl 40× NA 0.75 Ph2 lens (Olympus, Tokyo, Japan) with a high-speed CCD camera (IPX-VGA210LMCN or CLB-B0620M-TC000; Imperx, Boca Raton, FL) at 1,000 or 1,255 frames/s. Each captured image was transferred via a frame-grabber card (PIXCI-EB1; EPIX, Buffalo Grove, IL) to a computer for image analysis. This high-speed CCD camera was controlled by real-time video nanometry (RTVN) software, which we developed using LabVIEW 2009 (National Instruments, Austin, TX). Phase-contrast images of the beads were fitted by a two-dimensional Gaussian function for every sampling frame, and the position of a bead was expressed as *x* and *y* coordinates of a peak of fitted Gaussian curve. The bead position was approximated by an ellipse function every 500 frames, and the bead position was corrected to approximate a perfect circle centered on the origin. The rotation angle was calculated for every two sampling frames, and time traces of the angular velocity, rotational velocity, and rotational direction were estimated by repeating this process every video frame.

Protein localization assays. Cells were observed in microscope chambers like the ones used for motor rotation measurements. The cell suspension was loaded into the sample chamber and incubated for 15 min to allow the cells to attach to the coverslip. The inside of the sample chamber was gently perfused with 30 μL of 10NaMB to remove unattached cells. The fluorescence images of GFP-CheW and Venus-CheR were observed by IX71-based epifluorescence microscopy. A blue laser beam (Sapphire 488-20-SV; Coherent, Germany) was inserted into the microscope IX71. The blue laser beam was reflected by a primary dichroic mirror (FF495-Di02; Semrock, Lake Forest, IL) and focused on the back focal plane of the lens (APON 60XOTIRF NA1.49; Olympus, Tokyo, Japan). Fluorescence from the GFP or Venus fusion proteins was passed through the primary dichroic mirror and an emission filter (FF01-520/35, Semrock) and was focused on an electron multiplying charge-coupled device (EMCCD) camera (DU860D-CS0-BV; Andor Technology, UK). The fluorescent images were recorded at 0.5 frames/s, and EMgain was 100.

Correlation analysis. To analyze the switching correlation between flagellar motors, the rotational velocity was classified into three states by the following procedure (25). The time trace of the rotational velocity was filtered by the Chug-Kennedy filtering algorithm (C-K filter) (43), using an analytical window of 100 data points and a weight of 10. Rotational velocities of more than +20 Hz, between +20 Hz and −20 Hz, and less than −20 Hz were assigned as CCW rotation (+1), pause (0), and CW rotation (−1), respectively. The correlation analysis was performed by applying Equation 1 to the time traces of the rotational directions between two flagellar motors:

$$Z(\tau) = \frac{\frac{1}{N}\sum_{t=1}^{N}\left[x(t)\cdot y(t+\tau) - \overline{x(t)}\cdot\overline{y(t)}\right]}{\sqrt{\frac{1}{N}\sum_{t=1}^{N}\left[x(t)-\overline{x(t)}\right]^2}\cdot\sqrt{\frac{1}{N}\sum_{t=1}^{N}\left[y(t)-\overline{y(t)}\right]^2}} \quad (1)$$

where *Z* is the function used for the correlation analysis, *t* is time, τ is the time difference, *N* is the total number of sampling points, and *x*(*t*) and *y*(*t*) are the time traces of the rotational directions of two motors, respectively. Correlations *Z* (τ) were calculated ($-1 \leqq Z \leqq 1$) by Equation 1 using the traces of rotational direction from 60 to 120 s.

SUPPLEMENTAL MATERIAL

Supplemental material is available online only.

SUPPLEMENTAL FILE 1, PDF file, 3.3 MB.

ACKNOWLEDGMENTS

We thank Takeharu Nagai for the gift of plasmid encoding monomeric Venus.

This work was supported by Grants-in-Aid for Scientific Research 19H05797 (A.I., H.F., and Y.-S.C.) and 21K06097 (H.F.) from JSPS KAKENHI and by U.S. National Institutes of Health grant GM19559 (J.S.P.).

REFERENCES

1. Turner L, Ryu WS, Berg HC. 2000. Real-time imaging of fluorescent flagellar filaments. J Bacteriol 182:2793–2801. https://doi.org/10.1128/JB.182.10.2793-2801.2000.
2. Wadhams GH, Armitage JP. 2004. Making sense of it all: bacterial chemotaxis. Nat Rev Mol Cell Biol 5:1024–1037. https://doi.org/10.1038/nrm1524.
3. Macnab R. 1996. Flagella and motility, p. 123–145. *In* Neidhardt FC (ed), *Escherichia coli* and *Salmonella*. American Society for Microbiology, Washington, DC.
4. Parkinson JS, Hazelbauer GL, Falke JJ. 2015. Signaling and sensory adaptation in *Escherichia coli* chemoreceptors: 2015 update. Trends Microbiol 23:257–266. https://doi.org/10.1016/j.tim.2015.03.003.
5. Liu J, Hu B, Morado DR, Jani S, Manson MD, Margolin W. 2012. Molecular architecture of chemoreceptor arrays revealed by cryoelectron tomography of *Escherichia coli* minicells. Proc Natl Acad Sci U S A 109:E1481–E1488. https://doi.org/10.1073/pnas.1200781109.
6. Burt A, Cassidy CK, Ames P, Bacia-Verloop M, Baulard M, Huard K, Luthey-Schulten Z, Desfosses A, Stansfeld PJ, Margolin W, Parkinson JS, Gutsche I. 2020. Complete structure of the chemosensory array core signalling unit in an E. coli minicell strain. Nat Commun 11:743. https://doi.org/10.1038/s41467-020-14350-9.
7. Piñas GE, DeSantis MD, Cassidy CK, Parkinson JS. 2022. Hexameric rings of the scaffolding protein CheW enhance response sensitivity and cooperativity in

Escherichia coli chemoreceptor arrays. Sci Signal 15:eabj1737. https://doi.org/10.1126/scisignal.abj1737.
8. Fukuoka H, Sagawa T, Inoue Y, Takahashi H, Ishijima A. 2014. Direct imaging of intracellular signaling components that regulate bacterial chemotaxis. Sci Signal 7:ra32.
9. Stewart RC. 1997. Kinetic characterization of phosphotransfer between CheA and CheY in the bacterial chemotaxis signal transduction pathway. Biochemistry 36:2030–2040. https://doi.org/10.1021/bi962261k.
10. Sourjik V, Berg HC. 2002. Binding of the *Escherichia coli* response regulator CheY to its target measured *in vivo* by fluorescence resonance energy transfer. Proc Natl Acad Sci U S A 99:12669–12674. https://doi.org/10.1073/pnas.192463199.
11. Bren A, Eisenbach M. 1998. The N terminus of the flagellar switch protein, FliM, is the binding domain for the chemotactic response regulator, CheY. J Mol Biol 278:507–514. https://doi.org/10.1006/jmbi.1998.1730.
12. Welch M, Oosawa K, Aizawa S, Eisenbach M. 1993. Phosphorylation-dependent binding of a signal molecule to the flagellar switch of bacteria. Proc Natl Acad Sci U S A 90:8787–8791. https://doi.org/10.1073/pnas.90.19.8787.
13. Afanzar O, Di Paolo D, Eisenstein M, Levi K, Plochowietz A, Kapanidis AN, Berry RM, Eisenbach M. 2021. The switching mechanism of the bacterial rotary motor combines tight regulation with inherent flexibility. EMBO J 40:e104683. https://doi.org/10.15252/embj.2020104683.
14. Che YS, Sagawa T, Inoue Y, Takahashi H, Hamamoto T, Ishijima A, Fukuoka H. 2020. Fluctuations in intracellular CheY-P concentration coordinate reversals of flagellar motors in *E. coli*. Biomolecules 10:1544. https://doi.org/10.3390/biom10111544.
15. Cantwell BJ, Draheim RR, Weart RB, Nguyen C, Stewart RC, Manson MD. 2003. CheZ phosphatase localizes to chemoreceptor patches via CheA-short. J Bacteriol 185:2354–2361. https://doi.org/10.1128/JB.185.7.2354-2361.2003.
16. Vaknin A, Berg HC. 2004. Single-cell FRET imaging of phosphatase activity in the *Escherichia coli* chemotaxis system. Proc Natl Acad Sci U S A 101:17072–17077. https://doi.org/10.1073/pnas.0407812101.
17. Hazelbauer GL, Lai WC. 2010. Bacterial chemoreceptors: providing enhanced features to two-component signaling. Curr Opin Microbiol 13:124–132. https://doi.org/10.1016/j.mib.2009.12.014.
18. Rice MS, Dahlquist FW. 1991. Sites of deamidation and methylation in Tsr, a bacterial chemotaxis sensory transducer. J Biol Chem 266:9746–9753. https://doi.org/10.1016/S0021-9258(18)92884-X.
19. Han XS, Parkinson JS. 2014. An unorthodox sensory adaptation site in the *Escherichia coli* serine chemoreceptor. J Bacteriol 196:641–649. https://doi.org/10.1128/JB.01164-13.
20. Sourjik V, Berg HC. 2002. Receptor sensitivity in bacterial chemotaxis. Proc Natl Acad Sci U S A 99:123–127. https://doi.org/10.1073/pnas.011589998.
21. Li G, Weis RM. 2000. Covalent modification regulates ligand binding to receptor complexes in the chemosensory system of *Escherichia coli*. Cell 100:357–365. https://doi.org/10.1016/s0092-8674(00)80671-6.
22. Alon U, Surette MG, Barkai N, Leibler S. 1999. Robustness in bacterial chemotaxis. Nature 397:168–171. https://doi.org/10.1038/16483.
23. Barkai N, Leibler S. 1997. Robustness in simple biochemical networks. Nature 387:913–917. https://doi.org/10.1038/43199.
24. Yi TM, Huang Y, Simon MI, Doyle J. 2000. Robust perfect adaptation in bacterial chemotaxis through integral feedback control. Proc Natl Acad Sci U S A 97:4649–4653. https://doi.org/10.1073/pnas.97.9.4649.
25. Terasawa S, Fukuoka H, Inoue Y, Sagawa T, Takahashi H, Ishijima A. 2011. Coordinated reversal of flagellar motors on a single *Escherichia coli* cell. Biophys J 100:2193–2200. https://doi.org/10.1016/j.bpj.2011.03.030.
26. Cluzel P, Surette M, Leibler S. 2000. An ultrasensitive bacterial motor revealed by monitoring signaling proteins in single cells. Science 287:1652–1655. https://doi.org/10.1126/science.287.5458.1652.
27. Shiomi D, Zhulin IB, Homma M, Kawagishi I. 2002. Dual recognition of the bacterial chemoreceptor by chemotaxis-specific domains of the CheR methyltransferase. J Biol Chem 277:42325–42333. https://doi.org/10.1074/jbc.M202001200.
28. Banno S, Shiomi D, Homma M, Kawagishi I. 2004. Targeting of the chemotaxis methylesterase/deamidase CheB to the polar receptor-kinase cluster in an *Escherichia coli* cell. Mol Microbiol 53:1051–1063. https://doi.org/10.1111/j.1365-2958.2004.04176.x.
29. Wu J, Li J, Li G, Long DG, Weis RM. 1996. The receptor binding site for the methyltransferase of bacterial chemotaxis is distinct from the sites of methylation. Biochemistry 35:4984–4993. https://doi.org/10.1021/bi9530189.
30. Barnakov AN, Barnakova LA, Hazelbauer GL. 1999. Efficient adaptational demethylation of chemoreceptors requires the same enzyme-docking site as efficient methylation. Proc Natl Acad Sci U S A 96:10667–10672. https://doi.org/10.1073/pnas.96.19.10667.
31. Li M, Xu X, Zou X, Hazelbauer GL. 2021. A selective tether recruits activated response regulator CheB to its chemoreceptor substrate. mBio 12:e0310621. https://doi.org/10.1128/mBio.03106-21.
32. Feng X, Lilly AA, Hazelbauer GL. 1999. Enhanced function conferred on low-abundance chemoreceptor Trg by a methyltransferase-docking site. J Bacteriol 181:3164–3171. https://doi.org/10.1128/JB.181.10.3164-3171.1999.
33. Keegstra JM, Kamino K, Anquez F, Lazova MD, Emonet T, Shimizu TS. 2017. Phenotypic diversity and temporal variability in a bacterial signaling network revealed by single-cell FRET. Elife 6:e27455. https://doi.org/10.7554/eLife.27455.
34. Namba T, Shibata T. 2018. Propagation of regulatory fluctuations induces coordinated switching of flagellar motors in chemotaxis signaling pathway of single bacteria. J Theor Biol 454:367–375. https://doi.org/10.1016/j.jtbi.2018.06.023.
35. Shimizu TS, Aksenov SV, Bray D. 2003. A spatially extended stochastic model of the bacterial chemotaxis signalling pathway. J Mol Biol 329:291–309. https://doi.org/10.1016/s0022-2836(03)00437-6.
36. Krembel A, Colin R, Sourjik V. 2015. Importance of multiple methylation sites in *Escherichia coli* chemotaxis. PLoS One 10:e0145582. https://doi.org/10.1371/journal.pone.0145582.
37. Mears PJ, Koirala S, Rao CV, Golding I, Chemla YR. 2014. *Escherichia coli* swimming is robust against variations in flagellar number. Elife 3:e01916. https://doi.org/10.7554/eLife.01916.
38. Parkinson JS, Houts SE. 1982. Isolation and behavior of *Escherichia coli* deletion mutants lacking chemotaxis functions. J Bacteriol 151:106–113. https://doi.org/10.1128/jb.151.1.106-113.1982.
39. Ryu WS, Berry RM, Berg HC. 2000. Torque-generating units of the flagellar motor of *Escherichia coli* have a high duty ratio. Nature 403:444–447. https://doi.org/10.1038/35000233.
40. Datsenko KA, Wanner BL. 2000. One-step inactivation of chromosomal genes in *Escherichia coli* K-12 using PCR products. Proc Natl Acad Sci U S A 97:6640–6645. https://doi.org/10.1073/pnas.120163297.
41. Maloy SR, Nunn WD. 1981. Selection for loss of tetracycline resistance by *Escherichia coli*. J Bacteriol 145:1110–1111. https://doi.org/10.1128/jb.145.2.1110-1111.1981.
42. Sagawa T, Kikuchi Y, Inoue Y, Takahashi H, Muraoka T, Kinbara K, Ishijima A, Fukuoka H. 2014. Single-cell *E. coli* response to an instantaneously applied chemotactic signal. Biophys J 107:730–739. https://doi.org/10.1016/j.bpj.2014.06.017.
43. Chung SH, Kennedy RA. 1991. Forward-backward non-linear filtering technique for extracting small biological signals from noise. J Neurosci Methods 40:71–86. https://doi.org/10.1016/0165-0270(91)90118-j.

Supplemental Material

The chemoreceptor sensory adaptation system produces coordinated reversals of the flagellar motors on an *Escherichia coli* cell

Yumiko Uchida, Tatsuki Hamamoto, Yong-Suk Che, Hiroto Takahashi, John S. Parkinson, Akihiko Ishijima, Hajime Fukuoka

Table S1
Bacterial strains and plasmids

	Description	Reference
Strains		
RP437	Wild-type for motility and chemotaxis	38
UU2612	Δ*tar-tap* Δ*tsr* Δ*aer* Δ*trg*	44
EFS069	UU2612 *fliC-sticky*	This work
UU2610	Δ*tar-cheB* Δ*tsr* Δ*aer* Δ*trg*	44
EFS073	UU2610 *fliC-sticky*	This work
Plasmids		
pKG116	Cm^r P_{nahG}	45
pBAD24	Ap^r P_{BAD}	46
pBADKm	Km^r P_{BAD}	47
pPA114	*tsr* in pKG116	48
pFYC13	*tsr* Q297E (Tsr-EEQE) in pKG116	This work
pFYC15	*tsr* Q311E (Tsr-QEEE) in pKG116	This work
pFYC18	*tsr* Q297E/Q311E (Tsr-EEEE) in pKG116	This work
pFYC21	*tsr* E304Q/E493Q (Tsr-QQQQ) in pKG116	This work
pFYC23	*tsr* Q297E/E304Q/Q311E (Tsr-EQEE) in pKG116	This work
pFYC25	*tsr* Q297E/Q311E/E493Q (Tsr-EEEQ) in pKG116	This work
pUCI52	*tsr* Q297N/E304D/Q311N/E493D (Tsr-NDND) in pKG116	This work
pUCI30a	*tsr*ΔNWETF (deletion of 11 amino acids at the C-terminus) in pKG116	This work
pUCI23	*trg* in pKG116	This work
pUCI24	*trg*-NWETF (chimeric Trg fused with C-terminal 19 amino acid residues of Tsr) in pKG116	This work
pFSRB1	*cheR cheB* in pBAD24	This work
pFSRB4	*cheR*(R53A) *cheB*(H190Y) in pBAD24	This work
pUCI41	*cheR cheBc*(residues 147–349 of CheB, preceded by a start codon (Met)) in pBAD24	This work
pFSVnRB	*monomeric venus**[1]-*cheR cheB* in pBAD24	This work
pFSGW2	*egfp-cheW* in pBAD24	This work
pFYC37	*tsr*-3FLAG in pKG116	This work
pUCI44	*tsr*ΔNWETF-3FLAG in pKG116	This work
pUCI42	*trg*-3FLAG in pKG116	This work
pUCI45a	*trg*-NWETF-3FLAG in pKG116	This work
pUCI47c	*cheR*-3FLAG *cheB* in pBAD24	This work
pUCI48b	*cheR*(R53A)-3FLAG *cheB*(H190Y) in pBAD24	This work
pUCI49r	*cheR cheB*-3FLAG in pBAD24	This work
pUCI50	*cheR*(R53A) *cheB(*H190Y)-3FLAG in pBAD24	This work
pUCI51	*cheR cheBc*-3FLAG in pBAD24	This work

Ap^r, ampicillin-resistant; Cm^r, chloramphenicol-resistant; P_{lac}, *lac* promoter; P_{tac}, *tac* promotor; P_{BAD},

araBAD promoter; P_{nahG}, *nahG* promoter.

*[1]A gene for monomeric Venus was a gift from Prof. Takeharu Nagai.

In plasmids encoding Tsr mutants, the 5th methylation site in Tsr was always Glu (E) residue in this study, therefore the notation for the fifth site is omitted.

Supplemental method

Immunoblotting for MCP, CheR, and CheB variants.

EFS069 cells harboring expression plasmid encoding MCP variants were grown at 30°C for 5.25 h in TB containing salicylate described in Fig. S4A and 25 μg/mL chloramphenicol. Cells were harvested by centrifugation and then condensed by resuspending in 1× SDS loading buffer so that the optical density at 600 nm was 1 and were boiled at 95°C for 5 min. Whole-cell lysates were separated by SDS-PAGE using TXG FastCast polyacrylamide gel (#1610173, BioRad, Hercules, CA), and the proteins were detected by immunoblotting with an anti-FLAG antibody (F1804, SIGMA). Bands were detected with horseradish peroxidase (HRP) – conjugated anti-mouse antibody and the HRP conjugate substrate kit (#7076, CST, Danvers, MA).

EFS073 cells harboring pPA114 and expression plasmid encoding CheR and CheB variants were grown at 30°C for 5.25 h in TB containing 0.5 μM salicylate (for Tsr), 0.005% arabinose (for CheR and CheB variants), 25 μg/mL chloramphenicol, and 50 μg/mL ampicillin. Cells were harvested by centrifugation and then condensed by resuspending in 1× SDS loading buffer so that the optical density at 600 nm was 10 were boiled at 95°C for 5 min. Whole-cell lysates were separated by SDS-PAGE using 15% polyacrylamide gel, and the proteins were detected by immunoblotting with an anti-FLAG antibody. Bands were detected with HRP – conjugated anti-mouse antibody and the HRP conjugate substrate kit.

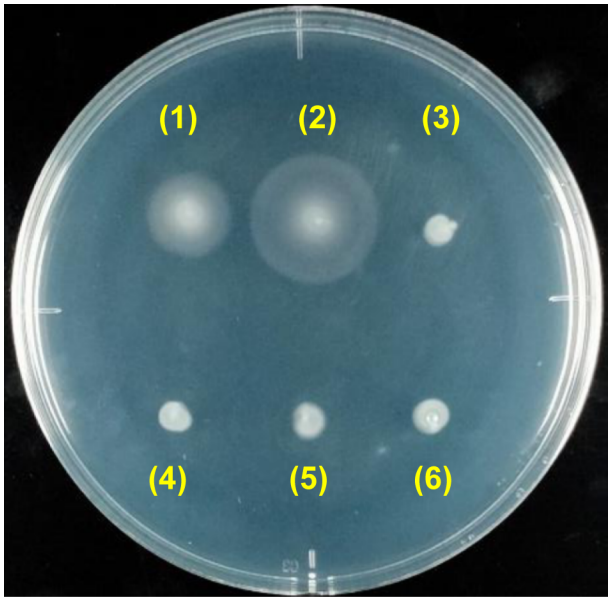

Figure S1. Chemotaxis of strains used to measure motor switching coordination. Cells were grown overnight at 30°C in LB medium containing 25 µg/mL chloramphenicol and 50 µg/mL ampicillin. Two microliter of an overnight culture was spotted onto TB-0.28% soft agar medium containing 0.5 µM salicylate to induce Tsr, 0.005% arabinose to induce CheR/CheB, 25 µg/mL chloramphenicol, and 50 µg/mL ampicillin. The plates were incubated at 30°C for 8 h. Note that all of these strains have sticky flagellar filaments, so the colonies spread more slowly than do those of strains with normal flagella.
Strain/plasmid combinations were (see Table S1 for genotype details):

(1) EFS073 / pPA114 (Tsr) / pFSRB1 (CheR/CheB)
(2) EFS069 / pPA114 (Tsr) / pBAD24 (empty vector) [CheRB expressed from EFS069 chromosome]
(3) EFS073/ pKG116 (empty vector) / pFSRB1 (CheR/CheB)
(4) EFS073 / pKG116 (empty vector) / pBAD24 (empty vector)
(5) EFS073 / pPA114 (Tsr) / pBAD24 (empty vector)
(6) EFS069 / pKG116 (empty vector) / pBAD24 (empty vector) [CheRB from EFS069 chromosome]

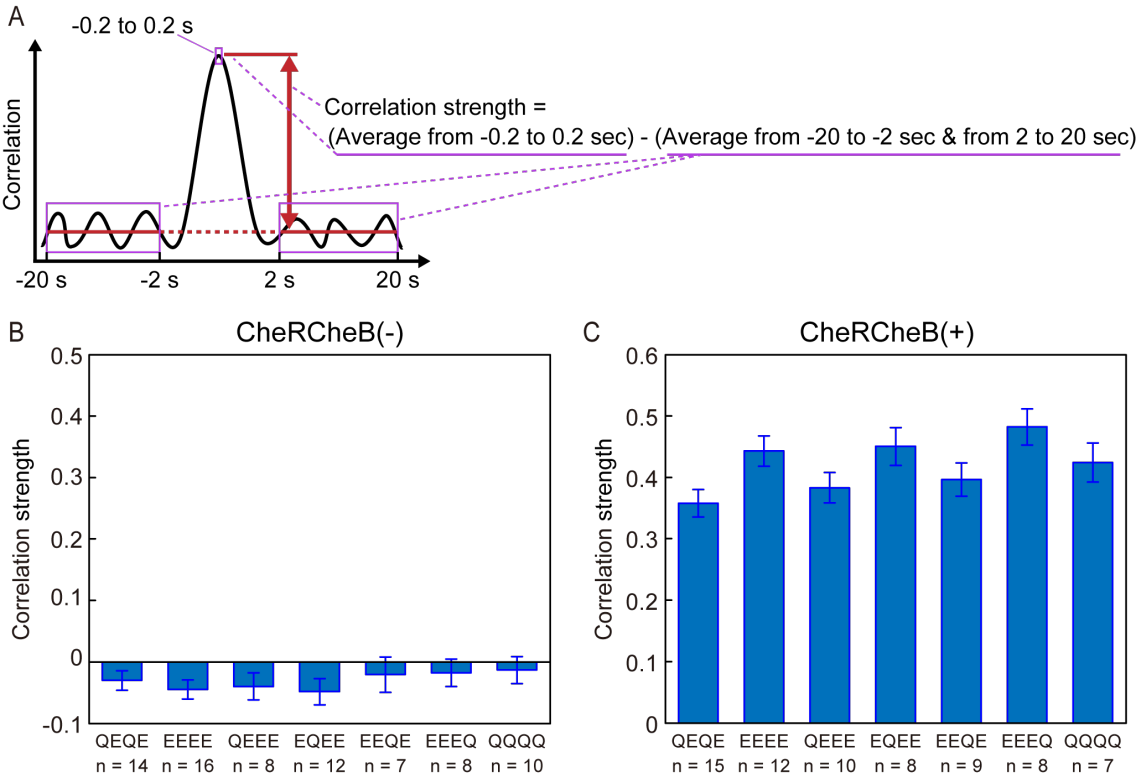

Figure S2. Rotational switching correlations in strains containing Tsr Q/E modification variants. (A) Correlation strength was defined as the difference between the peak-height and base-height of the correlation profile. The peak height was estimated as the average of values in the correlation profile from -0.2 to 0.2 seconds. The base height was estimated as the average of values from -20 to -2 seconds and from 2 to 20 seconds. (B) Correlation strength on an EFS073 cell carrying plasmids encoding a Tsr Q/E modification variant and pBAD24 (vector; no CheR or CheB). (C) Correlation strength on an EFS073 cell carrying plasmid encoding a Tsr Q/E modification variant and pFSRB1 (wild-type CheR and CheB). Error bar, standard deviation.

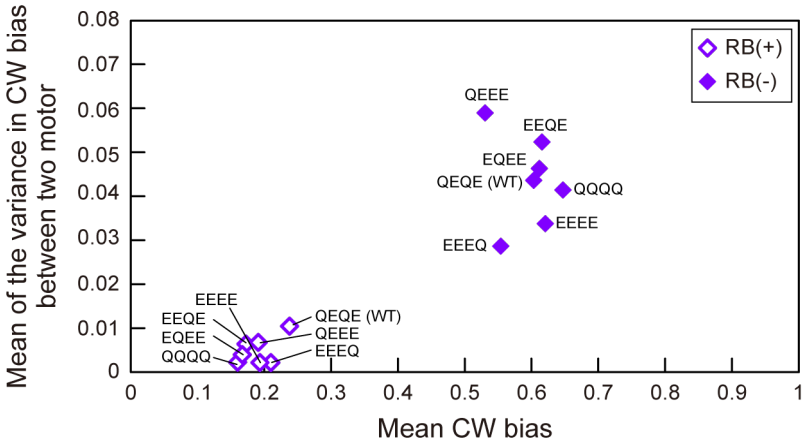

Figure S3. Relationship between CW bias and the variance in the bias between two motors of the same cell. In each strain containing a single Tsr Q/E variant, the mean CW motor bias is plotted on the x-axis and the mean of the variance between the two motors is plotted on the y-axis. Filled and open diamonds indicate CheRB(+) and CheRB(-) cells, respectively (the number of cells for each Q/E variant is the same as that presented in Fig. S2.).

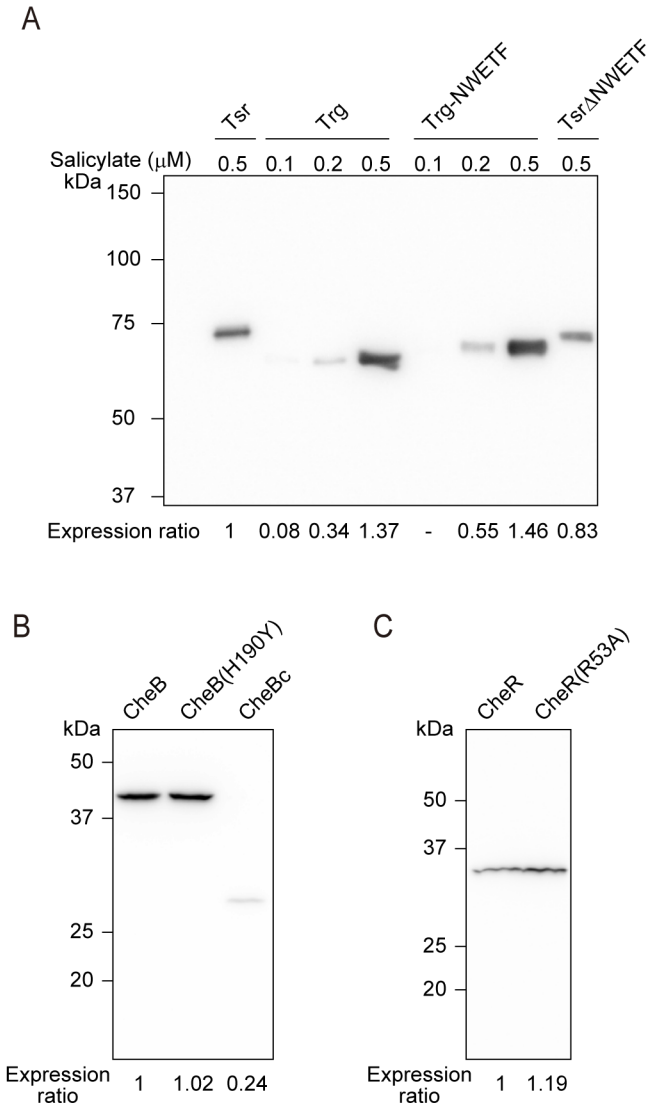

Figure S4. Cellular expression levels of FLAG-tagged derivatives of the proteins used in this study. Cell lysates were subjected to denaturing gel electrophoresis and proteins visualized by immunoblotting with anti-FLAG antibody. Positions of molecular weight marker proteins are shown on the kDa values on the left of each panel. Relative band intensities are listed below each panel. (A) MCP-FLAG variants. Salicylate concentrations (μM) for induction MCP variants are shown at the top. (B) CheR-FLAG variants. (C) CheB-FLAG variants.

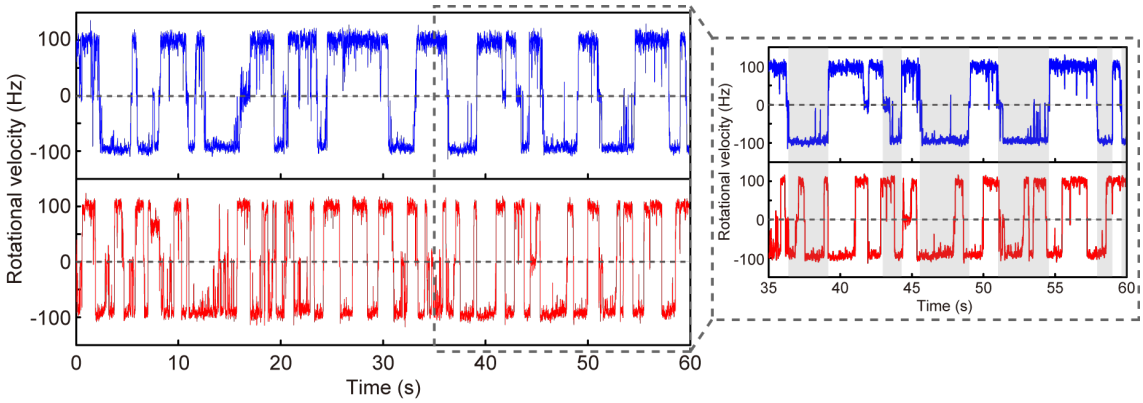

Figure S5. Long time traces of the rotational directions of two different motors on a cell producing Tsr wild-type [QEQE], CheR-R53A, and CheB-H190Y (see Fig. 3B). On the right, part of the trace record is shown on an expanded time scale. The gray area indicates periods of CW rotation of the motor in the upper trace.

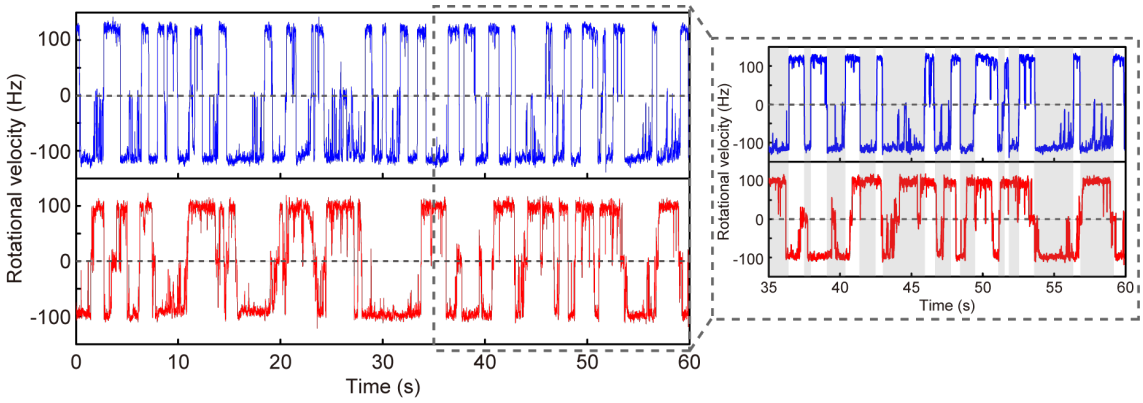

Figure S6. Long time traces of the rotational directions of two different motors on a cell containing Tsr [NDND], CheR, and CheB (see Fig. 4B). On the right, part of the trace record is shown on an expanded time scale. The gray area indicates periods of CW rotation of the motor in the upper trace.

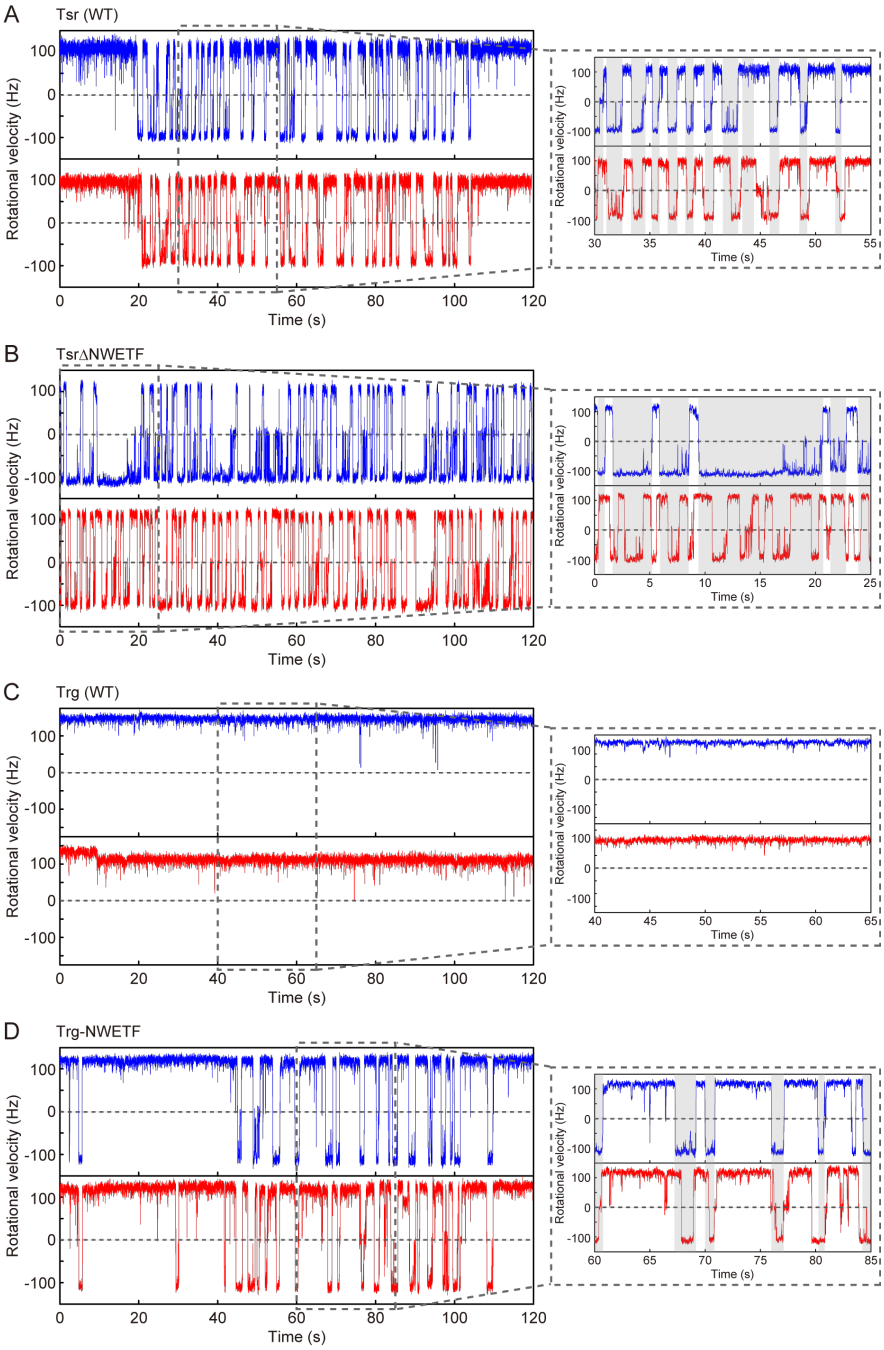

Figure S7. Long time traces of the rotational directions of two different motors on cells with various receptor variants (see Fig. 5). (A) Traces for wild-type Tsr in EFS069 (see Fig. 5C.) (B) Traces for TsrΔNWETF in EFS069 (see Fig. 5E). (C) Traces for wild-type Trg in EFS069 (see Fig. 5I). (D) Traces for Trg-NWETF in EFS069 (see Fig. 5J). On the right, part of the trace record is shown on an expanded time scale. The gray area indicates periods of CW rotation of the motor in the upper trace.

Supplemental references

44. Zhou Q, Ames P, Parkinson JS. 2011. Biphasic control logic of HAMP domain signalling in the Escherichia coli serine chemoreceptor. Mol. Microbiol. 80:596 – 611.
45. Gosink KK, Buron-Barral M, Parkinson JS. 2006. Signaling interactions between the aerotaxis transducer Aer and heterologous chemoreceptors in Escherichia coli. J. Bacteriol. 188, 3487–3493.
46. Guzman LM, Belin D, Carson MJ, Beckwith J. 1995. Tight Regulation, Modulation, and High-Level Expression by Vectors Containing the Arabinose PBAD Promoter. J. Bacteriol. 177, 4121–4130.
47. Fukuoka H, Inoue Y, Terasawa S, Takahashi H, Ishijima A. 2010. Exchange of rotor components in functioning bacterial flagellar motor. Biochem Biophys Res Commun. 2010 Mar 26;394(1):130-135.
48. Ames P, Studdert CA, Reiser RH, Parkinson JS. 2002. Collaborative signaling by mixed chemoreceptor teams in Escherichia coli. Proc. Natl. Acad. Sci. U. S. A. 99:7060–7065.